ORIGINAL ARTICLE

The Effects of Single and Bimetallic Silicon Composite Shields in Medical Imaging Methods: A Monte Carlo Study

Abbas Ali Nazeri [1], Reza Malekzadeh [1, 2], Parinaz Mehnati [2*] (ID) , Soheila Refahi [3*] (ID)

[1] Department of Medical Physics, School of Medicine, Tabriz University of Medical Sciences, Tabriz, Iran

[2] Medical Radiation Sciences Research Center, Tabriz University of Medical Sciences, Tabriz, Iran

[3] Department of Medical Physics, School of Medicine, Ardabil University of Medical Sciences, Ardabil, Iran

*Corresponding Authors: Parinaz Mehnati, Soheila Refahi
Email: parinazmehnati8@gmail.com, soheila52@yahoo.com

Abstract

Purpose: Nowadays, the use of polymer composites with several metals to design and build new radiation composite shields with practical features in radiology is expanding.

Materials and Methods: Three metal oxides, including Bismuth oxide (Bi_2O_3), Tungsten oxide (WO_3), and Tin oxide (SnO_2) were used as mono-metal and bimetallic compound silicon matrixes for clarification of their practical use. Monte Carlo simulation methods were used to enter the specifications of each metal in combination with silicon. The mass attenuation coefficients of the mono- and bimetallic composites were calculated in the energy ranges of 40 to 150 KeV by classification to low/ medium/high groups.

Results: The results showed the beam reduction ability for both the mono- and the bimetallic composites. The mass attenuation coefficients of Bi_2O_3, WO_3, and SnO_2 at 80 KeV were 0.38, 0.33, and 0.57 cm^2/gr, respectively. Moreover, the Bismuth-Tin bimetallic combination at low energies and the Bismuth-Tungsten at high energies had better attenuation than the other samples. To select bimetallic compounds with a high attenuation coefficient, it is better to match the energy used in the imaging method specifically. For example, in the 70-90 KeV energy range, the Sn-W combination had the highest beam attenuation coefficient.

Conclusion: The advantage of mono- and bimetallic shields in terms of energy attenuation amount depends on beam energy and shielding metal "K-absorption" edge. In comparing the attenuation of recorded beams in low, medium, and high ranges of energy, mono-metallic Bismuth shows higher attenuation coefficients than mono-metallic Tungsten and bi-metallic Bismuth–Tungsten. Dose reduction of the bi-metallic state of Bismuth - Tin was greater than that of mono-metallic Bismuth and Tin in low energies. Also, the attenuation of the Bi-Sn composite shield in low energy was the highest amount among all silicon composite shields.

Keywords: Bismuth; Tin; Tungsten; Nanocomposites; Computed Tomography Shields; Patient Radiation.

1. Introduction

In today's world, the use of X-ray machines, especially Computed Tomography (CT) imaging, in diagnosing various diseases is increasing. The main using new materials in therapy is for radio synthesizing of organs for radiation but in diagnosis goal is a lesser dose to the organ [1, 2]. The use of radiation, especially in CT scan is associated with an increase in the patient's radiation dose [3]. Any increase in radiation dose, especially in radiation-sensitive organs such as the breast, increases the possibility of delayed radiation effects, including cancer. Therefore, it is necessary to use a variety of radiation protection methods [4, 5]. One of the best and most effective ways to achieve radiation protection is to use a composite shield. A study has recently designed a belt composite shield, which shows promise as a protective device for reducing radiation risks to both the patient's breast and the operator during coronary angiography [6]. Because of the complications that arise with lead as the most common element used in radiation shields, the use of elements with a high atomic number and different radiation absorption properties such as Bismuth, Tungsten, and Tin has been proposed [7].

Using new materials to shield the patient from radiation in CT plays a main role in reducing the dose of radiation to the patient's sensitive organs, such as the breast. Many studies have examined using Bismuth shields. In one study, the use of Bismuth - silicone composite was studied in an attempt to reduce irradiation to the breast, and the image quality of the resulting images was also examined [8, 9]. The effect of irradiation, which concludes percentages of different metals on dose reduction in CT angiography, has been investigated for Bismuth shields [10]. The application of micro- and nano-sized Bismuth composite shields with different percentages was approved for CT scan and angiography radiation protection [11]. In review articles related to the study of energy, particle size, and types and combinations of metal particles as the composite, the effectiveness of each of these factors for Bismuth and Tungsten metals was assessed [12, 13]. Recent studies have shown that the type of polymer (silicon or polyurethane) has a significant effect on image noise levels in the case of Bismuth composite shields [14, 15]. In another study,

Tin was used as a matrix filler to absorb medium-energy photons in the X-ray spectrum, with excellent attenuation at the energy of 29 KeV [16]. Also, Tungsten has been one of the preferred metals for researchers to study radiation shields in recent years due to its high electron density compared to other elements [17, 18]. Movahedi *et al.* studied a dual composite shield made of Tungsten nano-oxide and Tin nano-oxide to investigate attenuation coefficients [19]. No study on tree-metallic compounds was found in the available references.

Considering all above-mentioned facts, many studies have investigated and designed composite shields with NPs. In this study, for the first time, we have used two methods (simulation and practical) to evaluate and design composite shields with three NPs. Therefore, the effects of radiation protection of composites containing Bismuth oxide (Bi_2O_3), Tungsten oxide (WO_3), and Tin oxide (SnO_2), NPs were investigated with Monte Carlo simulation. Then, a quantitative comparison of the mass attenuation coefficients (μ/ρ) of all simulated composites relative to each other with the focus on Bi_2O_3 as the material whose application is most studied compared with other materials in three groups of high, medium, and low energy in the ranges of medical imaging energies was performed.

2. Materials and Methods

2.1. Software

The Monte Carlo software used in this study was MCNPX5 code, which is used for simulation and protection ability analysis of radiation shields. The radiation shields were designed as composites which included a spherical metal amplifier enclosed in a cubic silicon matrix.

2.2. Shield Metals

Three metals, i.e. Bismuth, Tungsten, and Tin, (Bi_2O_3, WO_3, SnO_2) were selected as metal oxides to fill the matrix, with atomic numbers 83, 74, and 50, respectively, and K-absorption edges of 90.5, 69.5, and 39 KeV, respectively. These metals were used as the absorber for the low- and medium-energy photons in the X-ray spectrum. The filler metals with a

diameter of 100 nm were simulated as single and double metals used for placement in the matrix of the shields. Silicone rubber (density 1.11 g/cm^3) was used as the matrix polymer. Each composite contained 10% wt. of metal oxide and 90% wt. of silicon. Composite compounds in the energy range of 40 to 150 KeV with 10 KeV steps were simulated using the Tally f4 code.

2.3. Calculation Assay

The linear attenuation coefficient values were calculated using Lambert's law (Equation 1):

$$I(x) = I_0 e^{-\mu x} \tag{1}$$

Where (I_0) represents the intensity of the input beam, (I) represents the intensity of the output beam, (x) is the thickness of the absorber, and (μ) is the linear attenuation coefficient.

In each simulation, the ratio of the output beam to the input beam (I/I_0) was calculated in 3 thicknesses. By plotting the ratio of beam reduction to thickness (x) in Excel software, the linear attenuation coefficient was calculated as the slope of the resulting line diagram for each of the metal composites at a given energy. In the last step, the linear attenuation coefficient divided by the density of each compound gave the mass attenuation coefficient that was used as a parameter to compare the effects of composite shields.

2.4. Study Geometry

In designing the study geometry, the priority was to reduce the energy of the main beam by using two collimator plates with 5 cm apertures and placing a composite shield between them. According to the standards, this is a suitable distance between the source and the detector for removing the projected scattered rays. The general geometry of the simulation and the placement of silicon and metal in the composite in specific dimensions are shown in Figure 1A & B.

The general geometry of the simulation, shown in Figure 1A, shows the position of the source, 1st collimator (lead), composite shield, 2nd collimator (lead, and detector relative to each other. Figure 1B shows the parameters in this Figure including the structure of the shield simulation by showing the silicon and metal matrix inside it; a is the silicon matrix of the composite, b shows the size of the sphere for the metal of display, and d shows the protective thickness of the shield.

To investigate the behavior of the selected shields, according to the k edge of the metals, groups of low, medium, and high energy (L, M, and H, respectively) were selected. Group L comprised energies of 40, 50, 60, and 70 KeV; group M was composed of energies of 80, 90, 100, and 110 KeV; and group H comprised energies of 120, 130, 140, and 150 KeV.
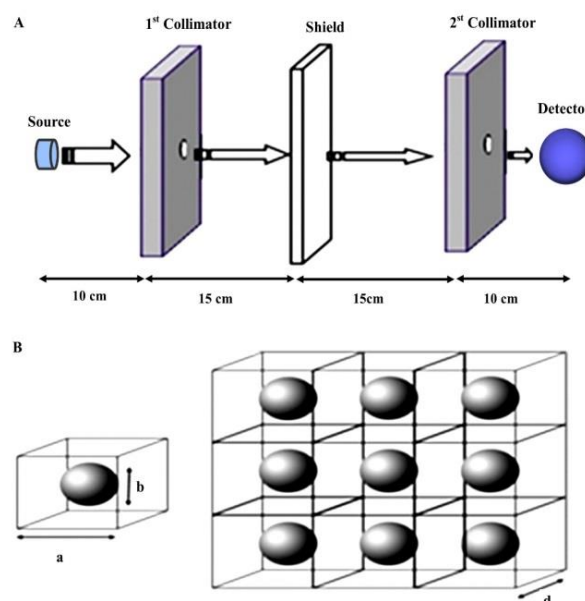

Figure 1. The general geometry of the simulation with Monte Carlo software. A: the position of the source, 1st collimator (lead), composite shield, 2st collimator (lead), and detector relative to each other, B: detail of shield simulation by showing the silicon and metal matrix inside it; a: is the silicon matrix of composite, b: shows the size of the sphere for the metal of display, and d shows the protective thickness of the shield

2.5. Validation of Advanced Code

The study employed a verification and validation process to assess the accuracy and credibility of the MC models used. The verification process involved comparing the MC results with data provided by XCom for pure bismuth and silicone. The linear attenuation coefficients of bismuth and silicone were calculated using the MC models and compared with established XCom data. This step ensured that the MC models accurately represented the behavior of bismuth and silicone shielding.

2.6. Fabrication of the Sample Composite Shield

After the synthesis of the fillers, the composites with 10% Bi_2O_3 weight were prepared using the compression molding technique. Liquid Silicon Rubber (LSR) with the chemical components of Si $(CH_3)O$ was selected as the matrix of the composites considering its beneficial properties for the production of radiation shields, particularly thermal and mechanical properties. In this method, the filler and LSR with appropriate proportions were sensitively weighed and mixed thoroughly for the fine dispersion of the filler in a mechanical stirrer for one hour at 50 rpm. Following that, they were dried at room temperature (25°C). Scanning optical microscopy was employed to evaluate the shape of the produced particles.

3. Results

3.1. Validation of Advanced Code

The validation of the simulation geometry was carried out by calculating the linear attenuation coefficients of

bismuth and silicone at photon energies ranging from 60-300 and 60-150 keV using the MCNPX code, respectively (Figure 2A, B). The results were then compared with the XCom data. The comparison showed a maximum difference of 1% between the calculated results and the XCom data, indicating the accuracy of the advanced MCNPX simulation geometry. Once the accuracy of the MC models was confirmed, the study proceeded to simulate the composites with the presence of metal Nanoparticles (NPs). The validated input codes were used to calculate the radiation mass attenuation coefficients of the samples, taking into account the influence of the metal NPs.

3.2. Bi_2O_3 and WO_3 Composite Shields

The mass attenuation coefficients of composite shields were calculated as mono- and bimetallic. Figure 3 shows the mass attenuation coefficients for the Bi_2O_3 and WO_3 single and double metal shields.

As shown in Figure 3, the attenuation coefficient for Bi_2O_3 single metal decreased with energy from 40 KeV before reaching the k-edge. At 90.5 KeV, an absorbed

Figure 3. The mass attenuation coefficients for single and double metal shields of Bi_2O_3, WO_3. μ/ρ: mass attenuation coefficient
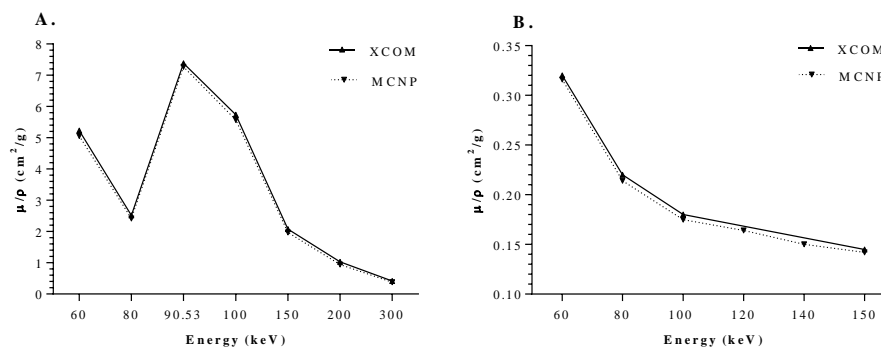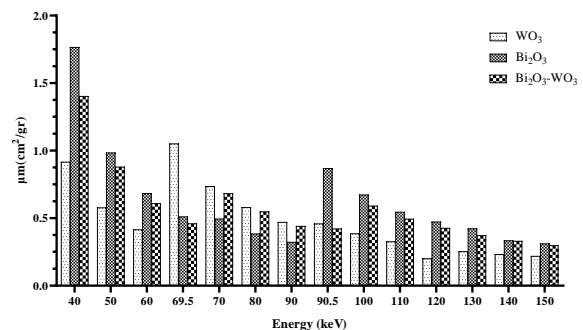

Figure 2. Mass attenuation coefficients of standard XCOM data compared to the MCNPX data for A: pure bismuth, B: pure silicon at various photon energies. μ/ρ: mass attenuation coefficient

peak was evident due to the k-edge energy; then the attenuation decreased again with increasing energy as observed in the area of energies M and H.

For WO_3 metal, in the energy range L and before its absorption edge, the attenuation rate decreased with increasing energy. When reaching the k-edge, absorption at the energy of 69.5 KeV was done; then an increase in beam absorption was observed. In the energy interval M, between the k-edge of the Bismuth and the end of the interval, the greatest attenuation was related to WO_3, which decreased with increasing beam energy. In the energy range H, the decreasing trend of the attenuating of this metal continued.

Changes in the absorption coefficient of the combined state of these two metals presented two increases in the energies related to the k edges (69.5 KeV and 90.5 KeV). Except for these two peaks related to the k edge, the adsorption coefficient decreased and was between the attenuation coefficients of monometallic states. In the ranges of low and high energies, its absorption was more than WO_3 and less than Bi_2O_3, and at energies of 140 and 150 KeV, it showed a parallel absorption with Bi_2O_3. Also in the energy range M, its attenuation rate is more than Bi_2O_3 but less than WO_3.

3.3. Bi₂O₃ and SnO₂ Composite Shields

Figure 4 shows the attenuation coefficients for the two metals Bi_2O_3 and SnO_2 as well as the shield obtained from combining these two metals. Bi_2O_3 attenuation is described in Figure 3. In the case of SnO_2 and with respect to the k edge of 39.5 KeV (which is less than the starting energy of the study), the highest attenuation coefficient was in L energies, and in the M and H groups, a relative decrease in mass attenuation coefficient was observed when the energy continued to increase.
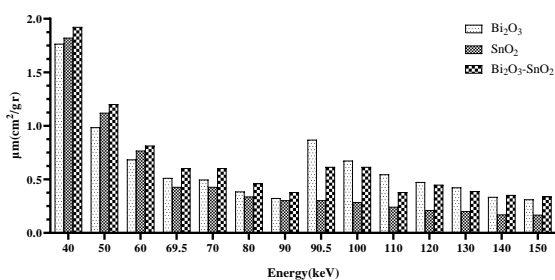

Figure 4. The mass attenuation coefficients for single and double metal shields of Bi_2O_3, SnO_2. μ/ρ:mass attenuation coefficient

3.4. WO₃ and SnO₂ Composite Shields

Figure 5 shows the attenuation coefficients of WO_3, SnO_2, and the composite shield of these two metals combined. The single metal attenuation states changed, as shown in Figures 1 and 3. WO_3 was lower than SnO_2 and higher than Bi_2O_3. After this region, the highest attenuation coefficient with a small difference compared to SnO_2 was related to the combined state of these two metals.
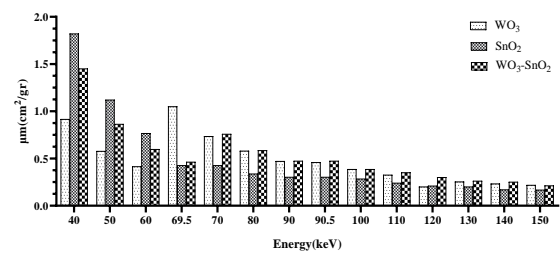

Figure 5. The mass attenuation coefficients for single and double metal shields of WO_3, SnO_2. μ/ρ:mass attenuation coefficient

3.5. Bimetallic Compounds

Figure 6 shows a general comparison of the bimetallic compounds. In the L and H energies, the greatest attenuation was related to Bi-Sn. In the L energies, Bi-W and W-Sn had the same mass attenuation coefficient. In the M range, no bimetallic compound had the highest attenuation, and due to the entry of the k edge Bi and W, increases in the attenuation coefficient were observed. At 70, 80, and 90 KeV, the W-Sn combination and the Bi-Sn combination had the most and least attenuation, respectively. At energies of 90 and 100 KeV, Bi-Sn had the highest beam attenuation coefficient, and at 110 KeV, W-Bi had more attenuation than other bimetallic compounds.
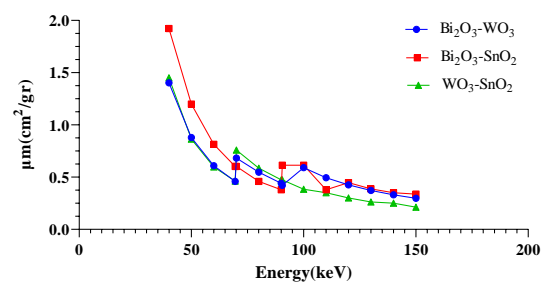

Figure 6. The mass attenuation coefficient for Bi_2O_3-WO_3, Bi_2O_3-SnO_2 and WO_3-SnO_2. μ/ρ:mass attenuation coefficient

A fabricated sample of nanoparticles, a Bismuth oxide shield, was performed and details for practical experiments for dosimetry of all shields will be done in future studies (Figure 7).
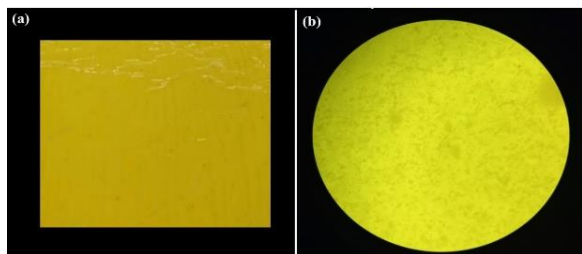

Figure 7. A fabricated sample of nanoparticles Bismuth (Bi_2O_3) shield. (a): photograph (b): light microscope

4. Discussion

The main purpose of this study was to investigate and compare shields made with Bismuth, Tungsten, and Tin metal oxide as mono-metals and combinations of two metals in the diagnostic radiology energy of CT scan and the amount of radiation absorbed in the three selected energy ranges.

Recently studies have shown that dose to organs during many types of CT scans leads to a 1.6 to 20.3 mSv effective dose according to the type of scanning and demographic properties of patients, thus using protection materials in CT scans recommended [20].

In the comparison of mono- and bimetallic shields, the response of bimetallic composite shielding cannot be considered as having the most or the least attenuation compared to mono. The importance of the k edge of metals as the boundaries of attenuation in composite compounds was also revealed. On the other hand, these new shields utilized k-edge photoelectric interactions as well as high photon absorption observed for photons with an energy range similar to k-shell binding energy. For example, as shown in Figure 3 in the bimetal compound Bi-W, between the two absorption edges marked P1 and P2 the observed highest mass attenuation coefficient was related to WO_3 (except for the high photon absorption in the Tungsten k-edge with 59% difference). Moreover, the difference between WO_3 and Bi_2O_3 absorption in this range was between 40% and 50%. Comparing Bi_2O_3 energy ranges (L to H), because of a difference of about 40% with WO_3 and about 10% to the bimetallic state, it seems that Bi_2O_3 will be a desirable choice in

the L range. Bi_2O_3 at the absorption edge k shows a double attenuation compared to other protectors. Furthermore, at energies higher than 90 KeV and in the H range, with a difference of more than 30% compared to WO_3 and about 10% compared to the bimetal state, it will be a good option to attenuate the beams used in medical imaging.

A higher attenuation coefficient was shown in the Bi-Sn bimetallic compound shield (Figure 4) than in the Bi_2O_3 and SnO_2 single metal state. Comparing the energy ranges in L and M, the superiority of the attenuation coefficient of the bimetallic compound compared to the mono-metallic state of Bi_2O_3 and SnO_2 with a difference between 5% to 29% was evident.

Due to the effect of the k absorption edge of the single metal beam of Bismuth oxide at energies higher than 90 KeV, the highest absorption was observed with a difference of about 50% compared to Tin and a difference between 5% and 40% compared to the bimetallic state. At 140 and 150 KeV, Bi-Sn bimetallic alloys showed a better attenuation than the Bi_2O_3 nanoparticle state by 4-7%.

For the compounds studied in Figure 4, the attention ability of the metal compounds of WO_3 and SnO_2 was: SnO_2> Sn-W> WO_3. A peak corresponding to the mass attenuation coefficient W was observed at the energy corresponding to the k absorption edge as the highest attenuation coefficient. The superiority of the WO_3 attenuation coefficient is evident in the energies after the k absorption edge. In a comparison of energy ranges, M indicated the suitability of using a combination of bimetallic and single metal WO_3 with a difference of less than 5%. In the energy range H, the superiority of the bimetal compound over each of the mentioned single metals was evident with a greater difference than the SnO2 attenuation coefficient.

To select the most effective bimetallic compounds for reducing attenuation in the range of medical imaging energies, a general comparison of the bimetallic compounds was performed (Figure 6). The results show the superiority of the compound Bi-Sn in the energy range L and H. Also, if we want to choose a two-metal compound with the same attenuation coefficient in the energy range L, both Bi-W and Bi-Sn metal compounds can be used. Another noteworthy point is the lack of well-defined behavior for

bimetallic compounds in the M range. To select bimetallic compounds with a high attenuation coefficient, it is better to match the energy used in the imaging method specifically. For example, in the 70-90 KeV energy range, the Sn-W combination had the highest beam attenuation coefficient.

In one study, 1% Bismuth in silicon matrix showed a reduction of 7% to 12% in the thickness of 1 mm and 1.5 mm for the dose of breast input in CT scan imaging and was recommended for use in CT imaging [21]. A comparison of linear attenuation coefficients with the present study showed the effect of metal weight percentage on the amount of attenuation coefficients. In energy 80 KeV, the attenuation coefficient to the mentioned research was 0.12 cm^{-1} and to the present study was 1.09 cm^{-1}.

In the micro-particles and Bismuth nanoparticles in the silicon matrix and in the energy range of diagnostic radiology (60-150 KeV), the effect of particle size on better attenuation properties was reduced by 11-18% and showed more beam in nano-mode [22]. There is an acceptable correlation between the results of the mass attenuation coefficient calculated for Bismuth metal during the mentioned study and the present one. The two studies are similar in the single-beam energy mode and energy range, particle size, and matrix, and both use the Monte Carlo simulator to calculate attenuation coefficients.

The results of the present study, which was performed on a 10% metal composite, showed the Bismuth - Tin bimetallic compound performed best in attenuating the beam in most of the studied energies, while Movahedi *et al.* [19] found that with a pure metal without considering the silicon composite, the best attenuation was Tungsten oxide (13.02%) and Tin oxide (73.78%). In the above study, by increasing the ratio of Tungsten in the composition, the amount (I/I_0) decreased. According to the results shown in Figure 4 and the absorption ratios of the three composites studied in this table in the energy range of 40-100 KeV, the results of the two studies can be considered to agree with each other.

Analysis of the results obtained in the present study and the mass attenuation coefficient calculated in the study by Hao Chai *et al.* [23] for Bismuth oxide and Tungsten metal showed similar reduction behavior and peaks at the Bismuth and Tungsten k-adsorption

edge, but they had less difference in absorption coefficients than the present study, which could be due to the effect of oxygen molecules on the structure of Bismuth oxide which, due to the lower absorption coefficient of this element compared to Bismuth, reduces the overall absorption coefficient and results in Tungsten. A study by a polyvinyl alcohol (PVA)/WO_3 composite, in the presence of high-energy gamma photons (662, 778, 964, 1112, 1170, 1130, and 1407 KeV), by Monte Carlo N-Particle simulation program presented that increasing of energy caused to a reduction of mass attenuation coefficient in both composite samples of micro-/nano-WO3 but coefficients and ability to shield are higher with nanocomposite [24]. In a comparison with our results, in energy ranges of 40-150 KeV, the amount of attenuation coefficient in the energies near the K-edge of tungsten (69.5 KeV) increased due to the photoelectric effect while for higher energies the amount of μ/ρ decreased due to Compton scattering and pair production which are two dominant events. Also, another study, using MCNP code, described a modified model to study the effect of size and proportion of tungsten (W) particles on the shielding properties of Light-Density Polyethylene (LDPE). Furthermore, they presented that the W proportion plays a more effective role than W size in attenuating gamma rays [25] that was completely approved in our study by different filler (Bi_2O_3, WO_3, and SnO_2) shielding properties. According to our media search, we did not find any study for single and bimetal, including a comparison of filler contains (Bi_2O_3, WO_3, SnO_2) by using MCNP code. Therefore, this study has a novelty for presenting in detail properties of single and bi-metal composites by MCNP methods. It seems performing simulation methods before practical fabrication of shields will be useful in correct selection of metal composite experiments as well as their economic fabrication.

5. Conclusion

The advantage of mono- and bimetallic protectors in terms of the amount of energy attenuation of the beam depends on the beam energy span and shielding metal "K" edge. In comparing the attenuation of recorded beams in low, medium, and high ranges of energy, mono-metallic Bismuth shows higher attenuation coefficients than mono-metallic Tungsten

and bi-metallic Bismuth-Tungsten. To select bimetallic compounds with a high attenuation coefficient, it is better to match the energy used in the imaging method specifically.

References

1- Behnaz Babaye Abdollahi *et al.*, "Main approaches to enhance radiosensitization in cancer cells by nanoparticles: A systematic review." *Advanced pharmaceutical bulletin,* Vol. 11 (No. 2), p. 212, (2021).

2- Sepehr Batooei, Amir Moslehi, and Jalil Pirayesh Islamian, "Assessment of metallic nanoparticles as radioenhancers in gastric cancer therapy by Geant4 simulation and local effect model." *Nuclear Instruments and Methods in Physics Research Section B: Beam Interactions with Materials and Atoms,* Vol. 488pp. 5-11, (2021).

3- P Mehnati and M Ghavami, "CT Role in the assessment of existence of breast cancerous cells." *Journal of Biomedical Physics & Engineering,* Vol. 10 (No. 3), p. 349, (2020).

4- R Smith-Bindman, J Lipson, and R Marcus, "Radiation dose associated with common computed tomography examinations and the associated lifetime attributable risk of cancer." *Journal of Vascular Surgery,* Vol. 51 (No. 3), p. 783, (2010).

5- Kyung-Hyun Do, "General principles of radiation protection in fields of diagnostic medical exposure." *Journal of Korean medical science,* Vol. 31 (No. Suppl 1), p. S6, (2016).

6- Reza Malekzadeh, Ali Tarighatnia, Parinaz Mehnati, and Nader D Nader, "Reduction of Radiation Risk to Cardiologists and Patients during Coronary Angiography: Effect of Exposure Angulation and Composite Shields." *Frontiers in Biomedical Technologies,* (2023).

7- Mahadevappa Mahesh, "Update on radiation safety and dose reduction in pediatric neuroradiology." *Pediatric radiology,* Vol. 45pp. 370-74, (2015).

8- Parinaz Mehnati, Reza Malekzadeh, Mohammad Yousefi Sooteh, and Soheila Refahi, "Assessment of the efficiency of new bismuth composite shields in radiation dose decline to breast during chest CT." *The Egyptian Journal of Radiology and Nuclear Medicine,* Vol. 49 (No. 4), pp. 1187-89, (2018).

9- Parinaz Mehnati, M Yousefi Sooteh, Reza Malekzadeh, Baharak Divband, and Soheila Refahi, "Breast conservation from radiation damage by using nano bismuth shields in chest computed tomography scan." (2019).

10- Parinaz Mehnati, Reza Malekzadeh, and Mohammad Yousefi Sooteh, "New Bismuth composite shield for radiation protection of breast during coronary CT angiography." *Iranian Journal of Radiology,* Vol. 16 (No. 3), (2019).

11- Parinaz Mehnati, Reza Malekzadeh, Mohamad Yousefi-Sooteh, and Farhad Yazdansetad, "Comparing X-ray dose reduction capability of silicon-bismuth micro- and nanocomposite shields using chest CT test." *Radiation Safety and Measurement,* Vol. 8 (No. 3), pp. 35-40, (2019).

12- Parinaz Mehnati, Reza Malekzadeh, and Mohammad Yousefi Sooteh, "Use of bismuth shield for protection of superficial radiosensitive organs in patients undergoing computed tomography: a literature review and meta-analysis." *Radiological physics and technology,* Vol. 12pp. 6-25, (2019).

13- Parinaz Mehnati, Reza Malekzadeh, and Mohammad Yousefi Sooteh, "Application of personal non-lead nano-composite shields for radiation protection in diagnostic radiology: a systematic review and meta-analysis." *Nanomed. J,* Vol. 7 (No. 3), pp. 170-82, (2020).

14- Parinaz Mehnati, Vida Sargazi, Zainab Yazdi Sotoodeh, Afshin Nejadjahantigh, and Masoome Farsizaban, "Introducing SRF in Bismuth-Silicon and Polyurethane shields for breast dose reduction during chest CT." *Journal of Complementary Medicine Research,* Vol. 11 (No. 5), pp. 195-95, (2021).

15- Parinaz Mehnati, Mehran Arash, and Parisa Akhlaghi, "Bismuth-silicon and bismuth-polyurethane composite shields for breast protection in chest computed tomography examinations." *Journal of medical physics,* Vol. 43 (No. 1), pp. 61-65, (2018).

16- Seyed Mohammad Javad Mortazavi, Alireza Zahiri, Daryoush Shahbazi-Gahrouei, Sedigheh Sina, and Masoud Haghani, "Designing a shield with lead-free polymer base with high radiation protection for X-ray photons in the range of diagnostic radiology using monte carlo simulation code MCNP5." *Journal of Isfahan Medical School,* Vol. 34 (No. 385), pp. 637-41, (2016).

17- Hajime Monzen *et al.*, "A novel radiation protection device based on tungsten functional paper for application in interventional radiology." *Journal of applied clinical medical physics,* Vol. 18 (No. 3), pp. 215-20, (2017).

18- NZ Noor Azman, SA Siddiqui, and It Meng Low, "Characterisation of micro-sized and nano-sized tungsten oxide-epoxy composites for radiation shielding of diagnostic X-rays." *Materials Science and Engineering: C,* Vol. 33 (No. 8), pp. 4952-57, (2013).

19- Mohammad Mehdi Movahedi *et al.*, "Novel paint design based on nanopowder to protection against X and gamma rays." *Indian Journal of Nuclear Medicine,* Vol. 29 (No. 1), pp. 18-21, (2014).

20- Hala Maher Ahmed, Mohamed Borg, Abd El-Aal Saleem, and Amira Ragab, "Multi-detector computed tomography in traumatic abdominal lesions: value and radiation control." *Egyptian Journal of Radiology and Nuclear Medicine,* Vol. 52 (No. 1), p. 214, (2021).

21- P Mehnati, M Arash, MS Zakerhamidi, and M Ghavami, "Designing and construction of breast shields using silicone composite of Bismuth for chest CT." *International Journal of Radiation Research,* Vol. 17 (No. 3), pp. 491-96, (2019).

22- Reza Malekzadeh, Parinaz Mehnati, Mohammad Yousefi Sooteh, and Asghar Mesbahi, "Influence of the size of nano-and microparticles and photon energy on mass attenuation coefficients of bismuth–silicon shields in diagnostic radiology." *Radiological physics and technology,* Vol. 12pp. 325-34, (2019).

23- Hao Chai *et al.*, "Preparation and properties of novel, flexible, lead-free X-ray-shielding materials containing tungsten and bismuth (III) oxide." *Journal of Applied Polymer Science,* Vol. 133 (No. 10), (2016).

24- F Kazemi and S Malekie, "A Monte Carlo study on the shielding properties of a novel polyvinyl alcohol (PVA)/WO3 composite, against gamma rays, using the MCNPX code." *Journal of Biomedical Physics & Engineering,* Vol. 9 (No. 4), p. 465, (2019).

25- Hoda Alavian and Hossein Tavakoli-Anbaran, "Study on gamma shielding polymer composites reinforced with different sizes and proportions of tungsten particles using MCNP code." *Progress in nuclear energy,* Vol. 115pp. 91-98, (2019).